INFLUENCE OF HX SIZE AND AUGMENTATION ON PERFORMANCE POTENTIAL OF MIXTURES IN AIR-TO-AIR HEAT PUMPS

C.K. Rice, Ph.D.

ABSTRACT

A modified Carnot analysis with finite heat exchanger (HX) sizes, counterflow HX configurations, and ideal glide matching was conducted for an air-to-air heat pump application. The purpose of the analysis was to determine the envelope of potential HX size and refrigerant-side augmentation benefits for ideal mixtures relative to pure refrigerant alternatives. The mixture coefficient of performance (COP) benefits examined are those due to exact external fluid glide-matching of idealized mixtures in more effective heat exchangers.

Maximum possible mixture COP gains are evaluated for four steady-state air-to-air heat pump conditions. Performance improvement opportunities are found to be primarily in the cooling mode. The effects of deviation from counterflow by use of crossflow and counter-crossflow HX configurations are addressed. Refrigerant-side augmentation with pure and mixed refrigerants is examined for air-side dominant and air-to-refrigerant balanced HXs.

INTRODUCTION

Advantages of HX Augmentation

The performance advantages of heat exchanger augmentation, in light of the growing urgency to switch to zero-ozone-depletion alternative refrigerants, are twofold. First, refrigerant-side augmentation can narrow the difference between pure and mixture heat transfer coefficients (Vineyard et al. 1992). Second, augmentation yields larger effective HX sizes, which increases the theoretical cycle advantage for nonazeotropic refrigerant mixtures (NARMs) over pure refrigerants (Didion and Bivens 1990) for applications where the external fluid temperatures are not constant through the heat exchangers (Lorenz 1894). Thus, for mixture cycles, there is a potential dual benefit from refrigerant-side enhancement.

Pure refrigerant alternatives (including azeotropes) will also benefit from HX enhancement by the incorporation of more efficient surfaces at the same time the heat exchangers are redesigned to accommodate a new fluid. Unless HX augmentation is sufficient to counter any reduced mixture heat-transfer coefficients and to offset mixture penalties for non-ideal HX configurations with improved cycle perfor-

mance, the comparative cycle COP gain from augmentation for NARMs may remain below that with pure refrigerant alternatives.

Objective of Present Analysis

The intent of this analysis is to provide an overview of the potential benefits of heat exchanger augmentation—with emphasis on the refrigerant-side—for pure and mixed refrigerants in air-to-air heat pumps. The analysis considers representative

— application source and sink temperatures,
— external fluid glides, and
— HX sizes referenced to known refrigerant-side conditions.

Approach

For the evaluation of HX augmentation benefits, the approach taken was first to determine the maximum potential COP gains from more effective heat exchangers, i.e., those with larger total (system) UA levels.[1] More effective heat exchangers can be obtained by increased air- and refrigerant-side surface areas, improved fin efficiency, increased tube-to-fin conductances, and/or enhanced air- and refrigerant-side heat transfer surfaces. We look initially at the benefits of more effective HXs without regard to the specifics of how such increases would be accomplished.

Following this more general evaluation for a range of typical operating conditions, we consider the effects of refrigerant-side heat transfer enhancement (and possible degradation in the case of mixtures).

MODIFIED CARNOT ANALYSIS WITH FINITE HEAT EXCHANGER SIZES AND FIXED EXTERNAL GLIDES

Simplifying Assumptions

A modified Carnot approach, using specified external fluid glides and HX mean temperature differences (MTDs)

---

[1] UA is defined as the overall conductance-area product for a heat exchanger.

C. Keith Rice is a research engineer at Oak Ridge National Laboratory, Oak Ridge, TN.

was used as the basis to assess the sensitivity of cycle COP to more effective HXs. Known refrigerant- and air-side conditions were used to establish baseline MTDs representative of an air-to-air heat pump. Both pure and mixed refrigerant cycles are analyzed with this MTD-based modified Carnot approach.[2]

The simplifying assumptions made for the analysis are as follows:

1. HX configurations are counterflow for mixtures—except where the effects of crossflow or counter-cross-flow configurations are explicitly considered;
2. there is exact glide matching for mixtures—refrigerant glides over evaporating and condensing regions exactly match the glides (i.e., ranges) of the respective external fluids giving linear, parallel temperature-vs.-length profiles[3];
3. pure refrigerants evaporate and condense at a constant temperature (no pressure drop effects considered);
4. cycle performance is based upon a first-law analysis of a modified Carnot cycle (in lieu of the vapor-compression cycle);
5. no refrigerant property effects (thermodynamic or transport) are considered in the cycle analysis or in the heat transfer analysis;
6. zero condenser subcooling and zero evaporator superheat are assumed; and
7. effects of changes in dehumidification performance are not considered.

With the above assumptions, cycle COP gains or losses due to the thermodynamic properties of specific refrigerants (such as the effects discussed by McLinden [1990]) are excluded. This allows the thermodynamics of the heat exchange process with finite size HXs to be examined independently. HX regions containing single-phase refrigerant (superheat in the evaporator and superheat and subcooling in the condenser) are assumed to be secondary issues and are also omitted from consideration.

Major Caveat Not considered in this analysis are the COP losses from the glide match limitations of any fixed-composition mixture relative to prescribed external temperature glides in a simple vapor-compression cycle. To approach exact glide matching in practice over both condenser and evaporator, a modified vapor-compression cycle, such as the solution circuit configuration proposed by Radermacher (1986), would be required.

The mixture COP benefits examined here are those solely due to exact external fluid glide matching of idealized mixtures in more effective HXs. These benefits can only be

partially attained with existing equipment; however, the assumptions serve to define the envelope of maximum mixture COP potential with finite heat exchanger sizes and representative air-side conditions.

Previous Work

A review of methods for the analytical comparison of pure and mixed refrigerants in vapor-compression cycles has been given by McLinden and Radermacher (1987). They have shown that the performance of mixtures relative to pure refrigerants is strongly dependent on how the equivalent temperature conditions were determined in the heat exchangers. Assumptions reported by McLinden and Radermacher ranged from specifying the same HX inlet, exit, mean, or dew-point refrigerant temperatures or the same total UA levels for the heat exchangers. McLinden and Radermacher recommended that a more meaningful comparison between pure and mixed refrigerants would maintain the same total heat transfer area (or total UA as an approximation) per unit of delivered capacity. The same external-fluid inlet and exit temperatures for the heat exchangers were also recommended.

The analysis conducted by McLinden and Radermacher (1987) and more recent work along these lines by Domanski and McLinden (1990), McLinden (1990), Rice and Sand (1990), and Jung and Radermacher (1991) included the effects of refrigerant thermodynamic properties and non-ideal glide matching for specific mixtures in HXs of fixed size and configuration. The present study applies the methodology recommended by McLinden and Radermacher (1987) to more idealized pure and mixed refrigerants over a range of total UA levels and HX configurations.

Basis for Modified Carnot Analysis

The adopted modified Carnot analysis is a variation and extension of an arithmetic mean temperature difference approach (AMTD) that was applied to water chillers by Kedzierski and Didion (1991). They used arithmetic averages to define the mean (midpoint) temperatures of the external fluids. The separation in midpoint temperatures between the external fluid and the refrigerant were used to represent the AMTDs for each heat exchanger. This approach yields true mean temperature differences (MTDs) for counterflow configurations where the refrigerant and external fluid glides match exactly.

AMTDs are only a rough approximation to the actual MTDs for the pure-refrigerant/finite-external-glide case. There, as shown in Figure 1, the refrigerant and external fluids tend to pinch at one end of the heat exchanger, and the external fluid temperature has a nonlinear asymptotic profile. The well-known log-mean-temperature difference (LMTD) equation (Holman 1972) can be used to determine the actual MTD given the pure refrigerant and external fluid temperatures. (Conversely, for an assumed MTD and external fluid conditions, the required pure refrigerant
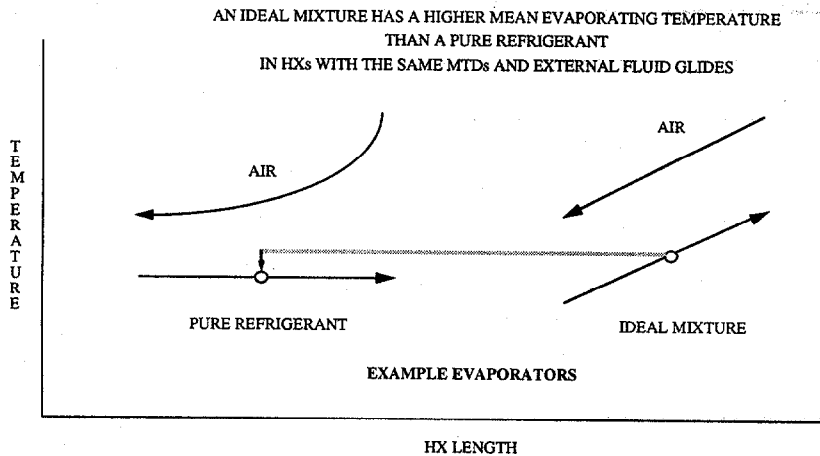
---

[2]A similar approach was described recently by Klein (1992) for use with pure refrigerants where the effectiveness/NTU method (Kays and London 1964) was used in the HX analysis.

---

[3]Two-phase refrigerant mixture temperature vs. enthalpy nonlinearity effects are also not considered.

AN IDEAL MIXTURE HAS A HIGHER MEAN EVAPORATING TEMPERATURE
THAN A PURE REFRIGERANT
IN HXs WITH THE SAME MTDs AND EXTERNAL FLUID GLIDES

Figure 1   *Heat exchanger temperature profiles for pure refrigerants and exact glide matching mixed refrigerants.*

temperature can be calculated.) Because the pure refrigerant has a constant evaporating or condensing temperature (assuming no pressure drop), the flow configuration is immaterial and the LMTD and the MTD are equivalent.

In the approximate approach, *the assumption of the same AMTDs* (instead of equal MTDs) *and the same external fluid glides for the pure and mixed refrigerant heat exchangers yields the same mean refrigerant temperatures.* This results in the prediction of equal modified Carnot cycle performance for pure and mixed refrigerant cycles, as shown in Figure 2, until a pinch point is reached for the pure case ($T_R = T_{X,OUT}$ at an AMTD of $\Delta T_X/2$ where ΔT_X is the external fluid glide).

At AMTDs below the pinch point, only the mixture calculation is relevant (in the AMTD approach) and only here does the mixture cycle show a potential performance increase from the larger effective HX area. An example of results obtained using this approach is shown in Figure 2 for a water-cooled chiller (Kedzierski and Didion 1991), where the external glides are 12°R (6.7 K) for each HX. This type of analysis is useful in showing that mixtures can benefit more from extremely large heat exchangers than can pure refrigerants. However, this representation also can be interpreted as showing that mixture cycles require much more heat exchanger area than is typically used in pure cycles to obtain any theoretical cycle benefit.

When the approximation of equal AMTDs is replaced by use of equal MTDs, *lower evaporating temperatures and higher condensing temperatures are obtained for pure refrigerants* compared to the equivalent glide-matching refrigerant case. This is shown conceptually in Figure 1 for evaporators where both pure refrigerant and ideal mixture cases have the same MTDs (same Q/UA and thereby the same HX loading) but where the mixture (Lorenz) case results in a higher mean refrigerant temperature. As a result, the *modified* Carnot COP (which is based on mean *refrigerant* temperatures) for the pure refrigerant cycle is always less than for the exact-glide-matching Lorenz cycle with equivalent heat exchangers and external glides. (In the

limit of zero external fluid glides, of course, the Lorenz and the Carnot cycles must become the same.) As heat exchanger size is increased (and MTDs are decreased), the differences in mean refrigerant temperature between the pure and mixed refrigerant cases increase and the COP advantage for the ideal mixture cycle increases.

Such behavior is consistent with the thermodynamic basis of the Lorenz cycle in that, for HXs with fixed MTDs and external glides, there is less irreversibility in the heat exchangers when the glides of the two heat exchanger streams are better matched (Herold 1989). This MTD-based modified Carnot COP calculation was adopted to assess the maximum potential benefits of more effective heat exchangers.
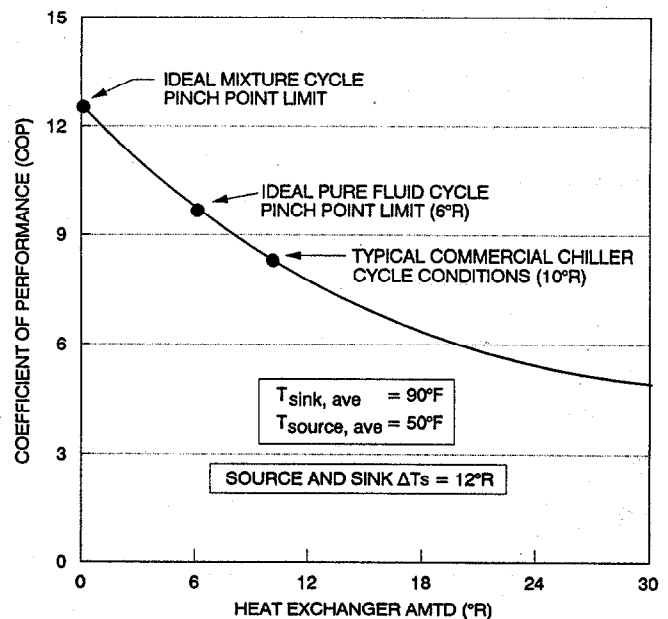

Figure 2   *Influence of heat exchanger effective size on cycle performance as predicted by a modified Carnot analysis based on arithmetic mean temperature differences (AMTDs).*

Equations for Modified Carnot COP

The standard relationship for a Carnot COP for a heat pump cycle is given by

$$COP_{CARNOT} = T_{DELIV}/(T_{SINK} - T_{SOURCE}) \quad (1)$$

where T_{DELIV} is the temperature of the delivered external fluid stream and

$$T_{DELIV} = T_{SOURCE}$$

for cooling and

$$T_{DELIV} = T_{SINK}$$

for heating and where the constant source and sink temperatures must be given on an absolute basis.

Mixed Refrigerant Mean Temperatures at Fixed MTDs

For the modified Carnot cycle of this analysis, the constant source and sink *external fluid* temperatures are replaced by mean *refrigerant-side* HX temperatures. For an air-to-air heat pump, T_{SOURCE} is replaced by $T_{E,MEAN}$ and T_{SINK} by $T_{C,MEAN}$ where $T_{E,MEAN}$ and $T_{C,MEAN}$ are the mean refrigerant temperatures in the evaporator and condenser, respectively. For the gliding refrigerant case, the air and refrigerant glides are assumed to match exactly:

$$T_{E,MEAN} = T_{SOURCE,AVE} - MTD_E/F \quad (2)$$

and

$$T_{C,MEAN} = T_{SINK,AVE} + MTD_C/F \quad (3)$$

where the mean source and sink temperatures, $T_{SOURCE,AVE}$ and $T_{SINK,AVE}$, are the arithmetic means[4] of the specified entering and leaving external fluid temperatures; MTD_E and MTD_C are specified condenser and evaporator mean temperature differences; and F is the LMTD correction factor (Holman 1972) for HX configurations other than counterflow ($F = 1$). The correction factors (F) for non-counterflow configurations can be determined from $\varepsilon/\varepsilon_{CF}$ at specified NTU, where ε and NTU are the HX effectiveness and number of transfer units as defined in Kays and London (1964) and the subscript CF refers to counterflow.

Pure Refrigerant Temperatures at Fixed MTDs

For the pure refrigerant case, the mean external fluid temperatures are given by a more complex relationship than an arithmetic average. In place of Equations 2 and 3 for ideal mixtures, pure refrigerant temperatures are determined

by an alternative expression that uses the known external fluid inlet and exit conditions and the basic LMTD equation (Holman 1972), which applies for any flow configuration when there is a constant-temperature fluid on one side. For a pure fluid, the LMTD equation reduces to

$$LMTD = MTD = (T_{X,IN} - T_{X,OUT})/ \\ [\ln\{(T_{X,IN} - T_R)/(T_{X,OUT} - T_R)\}] \quad (4)$$

where T_X and T_R are the external fluid and the refrigerant temperatures, respectively.

This equation can be solved for T_R of each HX as

$$T_R = T_{X,IN} + S \cdot \Delta T_X/(1 - e^{-Z}) \quad (5)$$

where $S = -1$ is for evaporating and $S = +1$ for condensing,

$$\Delta T_X = |(T_{X,IN} - T_{X,OUT})|,$$

and

$$z = \Delta T_X/MTD = NTU.$$

Equations 2, 3, and 5 are used in Equation 1 to calculate modified Carnot COPs for pure and mixed refrigerant cycles with equal MTDs and external fluid glides. Equation 5 is valid for pure refrigerants with all types of heat exchanger flow configurations, while Equations 2 and 3 for exact-glide matching mixtures are HX-configuration-dependent through the LMTD correction factor F.

Relating MTDs to Total System *UA*

Basic Equations Evaporator and condenser MTDs derived from given refrigerant-side conditions can be translated to levels of total heat exchanger *UA*. Individual HX MTDs[5] are related to the *UA* of each heat exchanger by the standard LMTD formulation of

$$Q = UA \cdot F \cdot LMTD = UA \cdot MTD \quad (6)$$

where MTD is equal to the LMTD that would result from a given heat transfer Q over a given *UA* in a counterflow configuration ($F = 1$). Because from Equation 6, MTD = Q/UA, it is a direct measure of the heat exchanger loading—the heat flux transferred per unit conductance. *By holding the MTD constant for a HX, the heat exchanger loading is thereby fixed.*

The reciprocal of the MTD is the amount of *UA* available per unit HX capacity, i.e.,

$$UA/Q = 1/MTD. \quad (7)$$

Normalizing to Unit Capacity Defining $(UA)_T = (UA)_E + (UA)_C$, the ratio $(UA)_T/Q_{DELIV}$ gives the total

---

[4]Alefeld (1987) has noted that entropically averaged source and sink temperatures (the exact mean temperature definition for use with the Carnot equation) *under exact glide matching* can be approximated by arithmetic averages when the ratios of absolute inlet to exit temperatures are close to unity—as is the case here.

[5]If a heat exchanger has more than one refrigerant region, such as superheated or subcooled regions, effective mean temperature differences (EMTDs) as described by Rice and Sand (1990) can be used instead of MTDs.

available UA per unit of delivered capacity (as in McLinden and Radermacher [1987]), i.e.,

$$(UA)_T / Q_{DELIV} = (UA)_T / Q_E$$

for cooling and

$$(UA)_T / Q_{DELIV} = (UA)_T / Q_C$$

for heating.

Using Equation 7, an expression for total UA available per unit of delivered cooling or heating capacity can be derived in terms of MTDs as

$$(UA)_T / Q_{DELIV} = \{ Q_E / \text{MTD}_E + Q_C / \text{MTD}_C \} / Q_{DELIV}. \quad (8)$$

For cooling, dividing through Equation 8 by Q_E (= Q_{DELIV}) gives

$$(UA)_T / Q_E = 1/\text{MTD}_E + (1/\text{MTD}_C) \cdot Q_C / Q_E, \quad (9)$$

and, similarly, for heating, Q_C (= Q_{DELIV}) gives

$$(UA)_T / Q_C = 1/\text{MTD}_C + (1/\text{MTD}_E) \cdot Q_E / Q_C \quad (10)$$

as applied by Rice and Sand (1990).

Temperature-Based Formulation For a modified Carnot-type analysis, the ratio of heat exchanger capacities in Equations 9 and 10 can be written as the ratio of their entropically averaged refrigerant temperatures (Alefeld 1987; Herold 1989), which are approximated here by their arithmetic means (Alefeld 1987), i.e., Q_E / Q_C becomes T_E / T_C. With this transformation, Equations 9 and 10 can be written as

$$(UA)_T / Q_E = 1/\text{MTD}_E + (1/\text{MTD}_C) \cdot T_C / T_E, \quad (11)$$

for cooling and

$$(UA)_T / Q_C = 1/\text{MTD}_C + (1/\text{MTD}_E) \cdot T_E / T_C, \quad (12)$$

for heating, or, in general, as

$$(UA)_T / Q_{DELIV} = \{ T_E / \text{MTD}_E + T_C / \text{MTD}_C \} / T_{DELIV} \quad (13)$$

where T_E and T_C are evaluated from Equations 2, 3, and 5.

The advantage in using $(UA)_T / Q_{DELIV}$, as given by Equations 11 through 13, instead of simply $(UA)_T$ can be seen by reference to Equation 13. By normalizing $(UA)_T$ to a per unit capacity basis, the effective total HX size is decoupled from the absolute temperature levels in the evaporator or the condenser and depends only on the ratio of temperature levels between the two heat exchangers. This ratio changes only slightly for the rather low-glide application considered here, and the MTDs for the pure and the ideal mixture cases are nearly the same.

By holding the value of $(UA)_T / Q_{DELIV}$ fixed, constant total (system) heat exchanger loading and a fixed unit

capacity can be maintained between the pure and mixed refrigerant cycles.

Evaluation of UA Multiples To evaluate performance for specified $(UA)_T / (UA)_{T,BASE}$ levels, the following procedure was followed. First, a baseline value of $(UA)_T / Q_{DELIV}$ was evaluated for the heat pump application using reference refrigerant conditions (as discussed in the next section) and the resulting ratio of condenser to evaporator MTD was determined. This MTD ratio was then maintained while the required MTDs to obtain larger total UA multiples were evaluated.

Because Q_{DELIV} is constant for the analysis, ratios of $(UA)_T / Q_{DELIV}$ values computed from Equation 13 yield $(UA)_T / (UA)_{T,BASE}$ multiples. For each desired UA multiple, an evaporator MTD was estimated, from which values of condenser MTD, T_E, and T_C were calculated from Equations 2, 3, and 5 and the resulting value of $(UA)_T / (UA)_{T,BASE}$ was determined.[6] This procedure was iterated until each specified UA multiple was obtained. At this point, the modified-Carnot COPs were calculated for the equivalently loaded, pure and mixed refrigerant conditions using Equation 1.

BASELINE CONDITIONS AND CONFIGURATIONS

An important part of any sensitivity analysis is the establishment of representative baseline conditions. With the methodology in place for evaluating the effect of increased UA level on the performance of pure and mixed refrigerant cycles, attention was focused on determining the range of effective HX sizes that exist in present air-to-air heat pump equipment relative to established refrigerant-side rating conditions for heat pumps. Representative refrigerant-side glides were also needed.

For this purpose, a survey was conducted of ARI members regarding representative external fluid glides (ranges), refrigerant-side conditions, and HX resistance ratios for heat pumps, chillers, and self-contained refrigeration systems (Hourahan and Hickman 1991).

For air-to-air heat pumps, data on middle- to top-of-the-line single-speed units were provided at 95°F (35°C) cooling and 47°F (8.3°C) heating conditions with some additional data on units of lower efficiency at 17°F heating (Rice 1992b).

---

[6]In the actual algorithm, the same MTD_E and MTD_C values were used for the pure and mixture cases, and two slightly different values of $(UA)_T / (UA)_{T,BASE}$ were obtained. These UA ratios were found to be within 1% of each other with the mixture value always slightly lower. This approximate approach was used because the difference was so small and because the effect gave a slightly conservative estimate of mixture potential. The more exact procedure would have been to maintain the same MTD on the HX delivering heating or cooling and to let the MTD on the other HX vary with the ratio of mean HX temperatures from Equation 13.

Range of Considered Refrigerant Conditions

The ARI-provided data gave a good representation of conditions for averaged middle-of-the line and state-of-the-art (SOA) units of the surveyed applications. To give the analysis a broader perspective, we chose to start the analysis with lower-efficiency baseline refrigerant conditions used as the standard compressor rating conditions (ARI 1990). From this lower-performance baseline, gains in effective heat exchanger size that have been made over the last decade or two, as represented by the ARI data, can be shown and compared to further improvements being considered. However, for the refrigerant-side augmentation benefits analysis, we will use the effective heat exchanger sizes computed for the ARI state-of-the-art conditions as the more appropriate reference point for comparison.

Baseline and State-of-the-Art Conditions for Air-to-Air Heat Pumps For air-source heat pumps, we chose the standard compressor cooling design condition of 45°F (7.2°C) evaporating and 130°F (54.4°C) condensing, as given in ARI (1990), as the lower-efficiency refrigerant baseline for the 95°F (35°C) ambient condition. To determine similar baseline refrigerant conditions for other heat pump ambient conditions, we used a combination of compressor rating conditions along with trend predictions of the ARI survey data and the MODCON heat pump design model (Rice 1991).

Results from the MODCON model were also compared with the ARI-provided external glides (i.e., ranges) to arrive at a set of representative glides for each of three considered ambient conditions and for single- and variable-speed conditions as appropriate. The selected glides are consistent with those used by Pannock and Didion (1991) and Pannock et al. (1992) in a screening study of single-speed heat pump alternatives. In contrast to the generally unequal external glides for air-to-air heat pumps, the external glides for the water-cooled chillers are usually the same for both heat exchangers but are smaller than for the air-to-air heat pumps, with typical values of 10°R (5.5 K).

The three ambients chosen for the air-to-air analysis were 95° and 82°F (35° and 27.8°C) in cooling and 35°F (1.7°C) in heating. Both single-speed and variable-speed conditions are considered at the 82°F (27.8°C) ambient in the cooling mode. For the heating mode, instead of the conventional 17° and 47°F (−8.3° and 8.3°C) ambient cases, we opted to consider only the intermediate temperature of 35°F (1.7°C), where both single- and variable-speed units would be operating at nearly the same capacity. This intermediate temperature was chosen as the temperature for which the major portion of the seasonal heating load is provided. Kondepudi and Bhalerao (1992) have also noted that the 35°F (1.7°C) rating point is the most influential of the heating-mode rating conditions on seasonal performance. Use of only one heating-mode temperature considerably simplified the heating-mode analysis (to one versus three possible conditions for single- and variable-speed units) and was deemed sufficient for the intended purpose.

The selected baseline refrigerant conditions and air-side (external fluid) glides for the air-to-air heat pump application are shown in Table 1. The external glides on the indoor coil are fairly constant at 21.5° to 22.5°R (11.9 to 12.5 K) for both heating and cooling, while the outdoor coil has smaller glides—ranging from 15°R (8.3 K) in cooling to half that for low-speed cooling and for the heating mode.

By using refrigerant saturation temperatures and air-side glides representative of a baseline heat pump operating at different conditions, the appropriate changes with ambient in unit capacity and thereby heat exchanger loadings and MTDs are included.

State-of-the-Art Air-to-Air Heat Pump Conditions In Table 2, refrigerant-side conditions for the low-efficiency baseline unit and the ARI medium- and high-efficiency cases at the 95°F (35°C) ambient condition are considered. The modified Carnot-cycle analysis was used to evaluate the respective MTDs for both HXs using the refrigerant conditions in Table 2 and the external glides from Table 1. Once the MTDs were evaluated from Equation 4, the total UA multiples relative to the baseline were evaluated using Equation 13.

The results shown in Table 2 indicate that the medium- and high-efficiency units have about 25% and 50% more effective total UA than for the traditional rating condition of 45°/130°F (7.2°/54.4°C). (A few ultra-high-efficiency systems, such as some of the recently introduced variable-speed systems, would have UA multiples near 1.75, while the postulated benchmark unit with refrigerant-side augmentation considered by Rice [1992a] is nearer a multiple of 2.0.) Based on these findings, a total UA multiple of 1.5 was adopted as the average state-of-the-art reference point for considering the benefits of refrigerant-side augmentation.

One other trend that can be seen from Table 2 is that the condenser MTDs have been reduced more proportionally than the evaporators as units with larger coils were introduced. The shift in condenser-to-evaporator MTD ratio to a value near unity for the state-of-the-art unit shows that more of the additional area has been directed to the outdoor coils.

Baseline and State-of-the-Art Air-to-Air HX Resistance Ratios The survey-requested HX resistance ratios were defined as the refrigerant-side-to-total heat transfer resistance ratios. This refrigerant-side resistance ratio, F_R, is given by

$$F_R = R_R/R_{HX} \qquad (14)$$

where $R_R = 1/(UA)_R$, $R_{HX} = 1/(UA)_{HX}$, and

$$1/(UA)_{HX} = 1/(UA)_R + 1/(UA)_X \qquad (15)$$

where the subscripts R, X, and HX refer to refrigerant-side, external-fluid-side, and overall HX values, respectively.

The values of F_R provided in the ARI data survey for unitary ACs and HPs ranged from 0.25 to 0.5 in cooling and from 0.3 to 0.6 in heating, with the condenser resis-

TABLE 1
Baseline Refrigerant and External Fluid Conditions for Air-to-Air Heat Pumps

Baseline Air-to-Air Conditions					
Ambient* °F (°C)	Speed Type	Base Sat. Temps. °F (°C)		External Glides °R (°K)	
		T_E	T_C	ΔT_E	ΔT_C
Cooling					
95 (35)	Single	45 (7.22)	130 (54.4)	21.5 (11.9)	15 (8.33)
82 (27.8)	Single	44 (6.67)	118 (47.8)	22.5 (12.5)	15 (8.33)
82 (27.8)	Variable	50 (10.0)	108 (42.2)	21.5 (11.9)	7.5 (4.17)
Heating					
35 (1.67)	Single/Variable	20 (-6.67)	104 (40)	7.5 (4.17)	22.5 (12.5)

*ARI Standard 210/240–89 indoor rating conditions of 80°F DB / 67°F WB (26.7/19.4°C) in cooling, 70°F (21.1°C) DB in heating

TABLE 2
Range of Derived MTDs and Total *UA* Levels for Air-to-Air Heat Pumps
at the 95°F (35°C) Ambient, Design Cooling Conditions

Air-to-Air HP at 95°F (35°C) Ambient					
Case	T_E °F (°C)	T_C °F (°C)	MTD_E °R (°K)	MTD_C °R (°K)	Total $UA_{relative}$
Low-Efficiency Baseline	45 (7.22)	130 (54.4)	22.6 (12.5)	26.8 (14.9)	1.0
ARI 10–11 SEER	49 (9.44)	125 (51.7)	18.2 (10.1)	21.6 (12.0)	1.24
ARI 11–13 SEER*	50 (10.0)	120 (48.9)	17.0 (9.44)	16.4 (9.1)	1.47

*Basis for selected UA multiple of 1.5 for SOA reference point

tance ratios generally being 0.05 to 0.1 higher than the evaporator.

BENEFITS OF INCREASED TOTAL *UA* AND REFRIGERANT-SIDE AUGMENTATION

With the baseline and state-of-the-art conditions established for the air-to-air heat pump application, the effects of total *UA* levels and refrigerant-side HX augmentation on cycle performance could be evaluated.
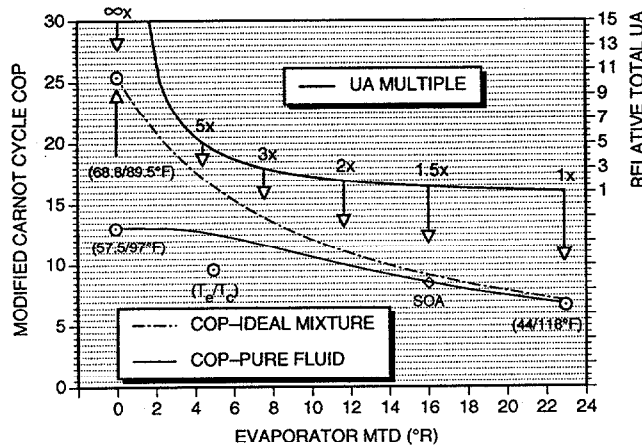
Benefits of Increased Total *UA*

The modified-Carnot COP approach described earlier was used to calculate comparative cycle COPs for pure refrigerant and idealized mixture systems. The cycle COPs are compressor-only values assuming a 100% efficient compressor. COP calculations were made for the four conditions considered for unitary air-to-air heat pumps. Before

summarizing the results from all the cases, an example of the use of this approach will be shown in more detail.

Air-to-Air Heat Pump, 82°F (27.8°C) Ambient, Single-Speed In Figure 3, the computed ideal cycle COPs are shown for pure and mixed refrigerant cases as functions of evaporator MTD. The conditions (from Table 1) and assumptions for the analysis are summarized in the figure legends. The baseline 44°F/118°F (6.7°C/47.8°C) condition identified in Figure 3 for the 82°F (27.8°C) ambient condition is (from Table 1) equivalent in total HX area to the standard 45°F/130°F (7.2°C/54.4°C) condition (ARI 1990) at the 95°F (35°C) ambient.

The associated multiples of total HX *UA* (over both coils) are overlaid on the plot to relate the increase in *UA* multiple to the widening difference between COPs predicted for the pure constant-temperature refrigerant versus the exactly glide-matching mixture. The ideal mixture advantage is seen to be small at *UA* levels between the 1X baseline and the 1.5X state-of-the-art values. At *UA*

Figure 3   *Effect of HX MTDs and total UA levels on the performance of pure fluid and ideal mixture cycles—air-to-air heat pump, 82°F (27.8°C) ambient, single-speed.*

multiples greater than 2X, the pure refrigerant case shows rapidly diminishing returns as the limiting pinch-point condition of 57.5°F evaporating/97°F condensing (14.2°C/36.1°C) is approached. For the ideal mixture, the limiting *mean* refrigerant temperatures are considerably closer together at 68.8°F evaporating and 89.5°F condensing (20.4°C/31.9°C).

As heat exchanger size is increased (as the MTDs are decreased for the same HX capacity), the modified-Carnot COP advantage for the mixture is seen to accelerate toward a maximum at infinite HX area. However, a not insignificant theoretical advantage also exists at heat exchanger sizes at and below the 2X *UA* multiple, which is near the predicted pure-refrigerant pinch point[7] from the more approximate AMTD analysis.

A comparison of Figure 3 to Figure 2 (where the abscissa of AMTD is comparable to MTD) shows that the MTD-based analysis provides a more definitive basis for comparing pure to mixed refrigerant performance. The MTD-based analysis separates the pure and mixed refrigerant COP curves throughout the *UA* range (as determined by the difference in mean HX temperatures calculated by Equation 5 versus that from Equations 2 and 3).

In addition to the COP separation at the lower *UA* levels, the extended asymptotic curve for the pure refrigerant also provides a more accurate basis for calculating COP

---

[7]The pinch point from the AMTD approach would be at 11.25 F° evaporator MTD in Figure 3.

gain potential for the mixture cases at the intermediate *UA* levels (past 2X multiples). The AMTD method would use the COP at near the 2X condition for this calculation and thus would overestimate the mixture advantage at intermediate *UA* levels. This intermediate range is of significant interest in augmentation assessments in addition to the 1.5 to 2X region.

The 82°F (27.8°C) ambient, single-speed condition was selected from among the air-to-air cases as the condition with the greatest mixture potential to be realized in practice. This is because of

1. the possibility of operating at a low pressure ratio at this condition since the source and sink temperatures are so close (82°F [27.8°C] outdoor vs. 80°F [26.7°C] indoor) and

2. the favorable relative size of the glides in the evaporator and condenser (22.5°R [12.2 K] evaporator and 15°R [8.3 K] condenser), which could be rather closely approached in a real mixture without requiring more elaborate means to adjust the refrigerant glide.

Since the 82°F (27.8°C) condition is the basis for the SEER calculation for both heat pumps and air conditioning, this condition is equally applicable for both types of equipment.

Effects of HX Flow Configuration The ideal mixture results shown in Figure 3 apply only for counterflow HX configurations whereas the pure refrigerant results are independent of flow configuration. The degree to which air-to-refrigerant HXs in a reversible heat pump approach counterflow in heating and cooling mode operation requires further examination.

Considered Configurations To assess the range of possible effects due to nonideal flow configurations that are more representative of existing air-to-refrigerant HXs, appropriate equations were implemented for computing the LMTD correction factors (F) for typical departures from counterflow. Possible circuiting arrangements are shown in Figure 4, where three configurations—alternating, crossflow, and cross-counterflow—are ordered by their increasing approach to counterflow. These configurations are:

*   Type A—alternating circuiting containing parallel and counterflow sections. This configuration was not modeled in the present analysis because the parallel sections would not be appropriate for use with gliding mixtures.
*   Type B—single-pass crossflow with both fluids unmixed as represented by Hiller and Glicksman (1976) by a curve fit to the numerical solution shown graphically by Kays and London (1964). This configuration is often used in heat pumps because the flow arrangement stays the same when the refrigerant flow is reversed between heating and cooling modes.
*   Type C—counter-crossflow with air-side unmixed, refrigerant-side mixed, and the unmixed passes in invert-

TYPE A	TYPE B	TYPE C
ALTERNATING CONFIGURATION	CROSSFLOW	CROSS-COUNTERFLOW
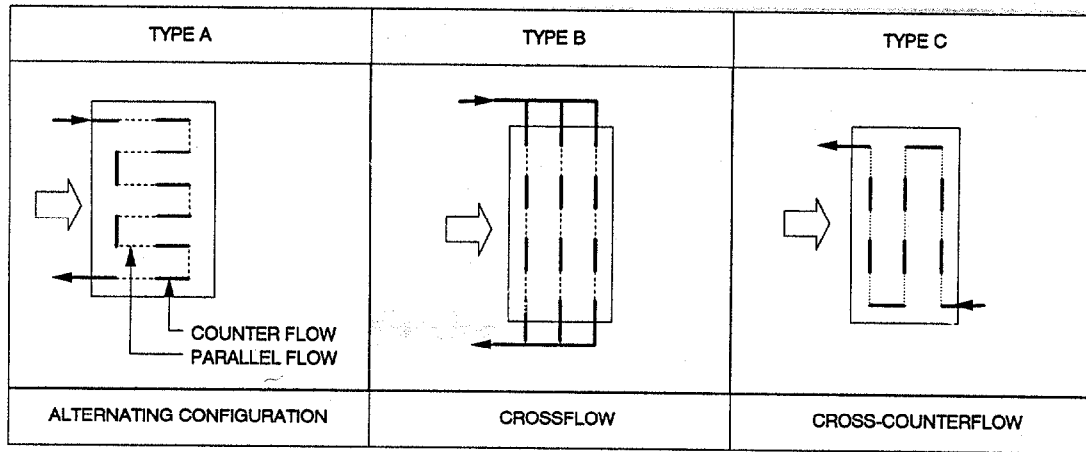
Figure 4   *Some possible circuiting arrangements for air-to-refrigerant heat exchangers in air-to-air heat pumps—ordered by increasing approach to counterflow.*

ed order as defined by Stevens et al. (1957). This is a most desirable circuiting arrangement for unidirectional operation such as in an air-conditioning-only unit.

The Type-B single-pass configuration shown in Figure 4 with three parallel rows (single-pass) is only an approximation to the *many-row* (single-pass) crossflow solution given by Kays and London (1964) with both fluids unmixed. As such, the many-row crossflow solution will predict more optimistic results than a crossflow coil with few rows (with the same limiting case solution for one-row as the cross-counterflow case).

Counter-crossflow configuration performance (Type-C) is evaluated here for one-, two-, three-, and many-row (many-pass) cases (per the equations of Stevens et al. [1957]), while the crossflow arrangement is determined only for the many-row and the one-row cases.[8]
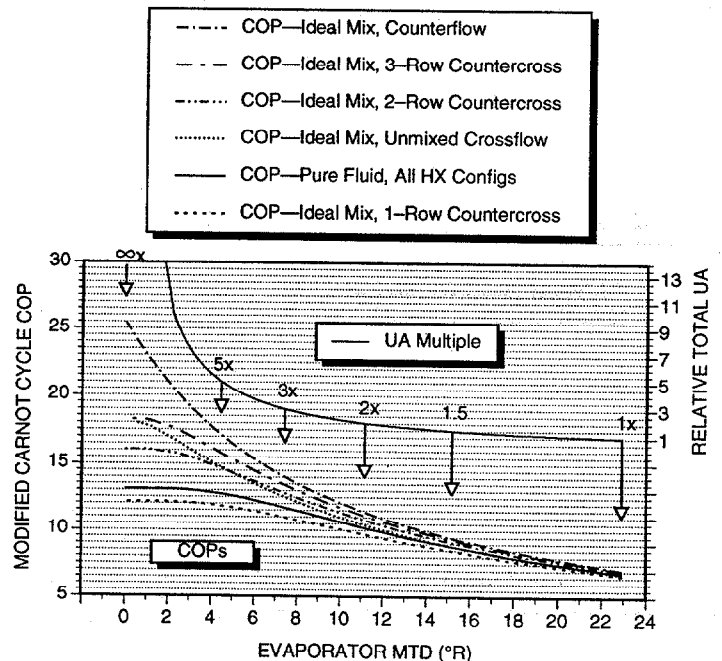
The Type A configuration shown in Figure 4 should perform more poorly than any of the configurations considered with mixtures, except perhaps the one-row configuration, because of the alternating parallel-flow and counterflow passes.

Performance with Different HX Configurations The comparative COP results using these nonideal flow configurations for both heat exchangers are shown in Figure 5. There the HX configuration cases are ordered in the legend in the approximate ranking of increasing performance. With a one-row counter-crossflow (or crossflow) HX, the COP of the ideal mixture is seen to fall below the pure fluid COP for all HX sizes with a maximum of about 8% loss in COP. A two-row counter-crossflow configuration reduces the losses of the one-row case (relative to the mixture with counterflow) by about 50% with all mixture COPs remaining above the pure fluid case.

Relative COP Gains with Different HX Configurations In Figure 6, the results of Figure 5 have been replotted in terms of percentage COP gain as a function of relative system *UA* multiple. The mixture COP gains (or losses) are referenced to the pure fluid COPs at the same *UA* levels. Potential mixture gains are seen to range from +4% to

Conditions:
ARI 82°F Ambient, Single-Speed
22.5°R Evap, 15°R Cond Glides
Baseline Refrig. Conditions $-T_e/T_c = 44/118$°F

Assumptions:
Fixed External Glides
Exact Glide Matching With Mixture
Fixed Cond/Evap MTD Ratio of 1.2

— · — · COP—Ideal Mix, Counterflow
— — — COP—Ideal Mix, 3–Row Countercross
— · · — · · COP—Ideal Mix, 2–Row Countercross
· · · · · · · · · COP—Ideal Mix, Unmixed Crossflow
———— COP—Pure Fluid, All HX Configs
· · · · · · COP—Ideal Mix, 1–Row Countercross

Figure 5   *Effect of HX MTDs, total UA levels, and flow configuration on the performance of pure fluid and ideal mixture cycles—air-to-air heat pump, 82°F (27.8°C) ambient, single-speed.*

[8]The one-row *cross*flow case is equivalent to the one-row *counter-cross*flow case.
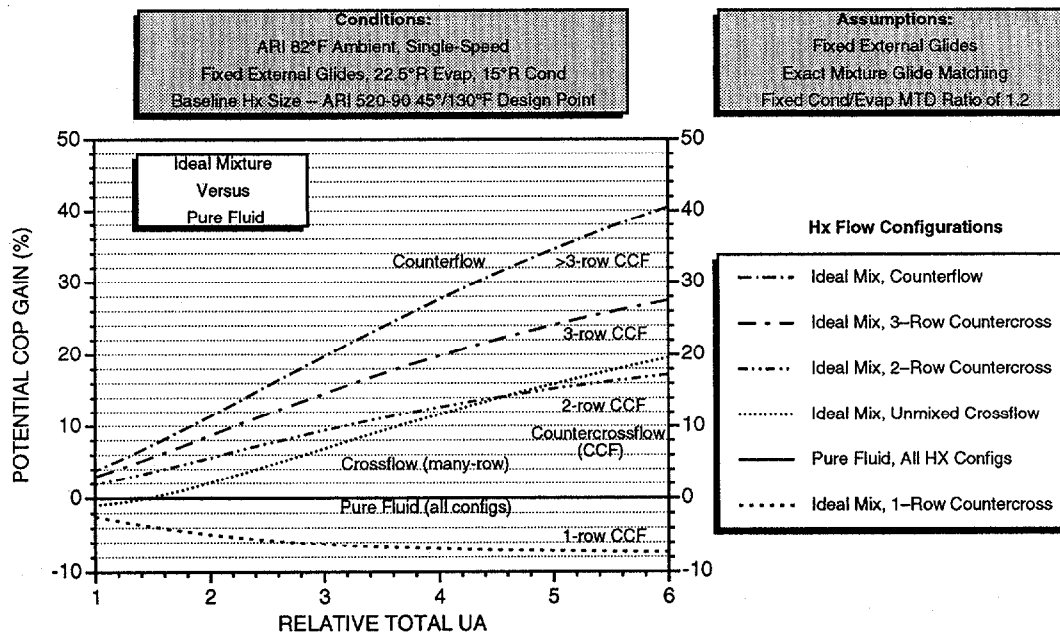
Figure 6 *Effect of relative UA levels and flow configuration on potential COP gains of ideal mixtures—air-to-air heat pump, 82°F (27.8°C) ambient, single-speed.*

−2% at the baseline low-efficiency *UA* multiple and from +40 to −8% at six times baseline size (four times state-of-the-art *UA* levels) depending on whether counterflow or one-row refrigerant-side-mixed, air-side-unmixed configurations are assumed. The possible performance envelope for ideal mixtures in a counter-crossflow arrangement is quite broad between one and four rows. The performance range for ideal mixtures in crossflow is half as wide for *UA* levels less than three times the baseline size.

The many-row unmixed crossflow case performs more poorly than a two-row counter-crossflow arrangement for *UA* multiples of most interest, i.e., less than three times the baseline (or twice the state-of-the-art *UA* levels). Only above *UA* multiples of four times the baseline does the many-row unmixed crossflow approach finally outperform the two-row counter-crossflow case. Below the state-of-the-art *UA* level, an ideal mixture in many-row crossflow only approaches pure fluid performance. (How well the *few*-row configurations such as Type B of Figure 4 approach the *many*-row unmixed crossflow results remains to be analyzed.)

With three rows of counter-crossflow refrigerant circuiting, mixture performance gains are 75% or more of the counterflow case until the *UA* multiples are greater than three times the base *UA* level. Stevens et al. (1957) notes that a four-row counter-crossflow configuration so closely approaches the results for counterflow that no further distinction should be necessary for most purposes.

The losses from many-row crossflow performance relative to counterflow are seen to eliminate or sharply reduce most of the mixture COP gains until UA multiples of twice the state-of-the-art HX size are reached. Few-row crossflow configurations will have a further reduction in

relative performance. *A counter-crossflow arrangement with two rows is seen to outperform a many-row crossflow arrangement* at *UA* multiples of most practical interest. From Figure 6, one can further deduce that this same two-row counter-crossflow arrangement (for both coils) would also outperform a unit with a one-row outdoor coil (a common configuration) combined with a four-row counter-crossflow indoor coil.

With proper design and unidirectional refrigerant flow, heat exchangers with three to four rows can be circuited to yield close to counterflow performance. Alternatively, *a two-row counter-crossflow outdoor coil combined with a four-row counter-crossflow indoor coil could exceed 75% of the performance potential predicted for heat pumps with counterflow HXs.* Because the indoor coil has the larger external glide, a greater benefit will be obtained from a closer approach to counterflow on this heat exchanger.

For reversible heat pump operation (where the refrigerant flow direction reverses between the heating and cooling modes), some circuit reversal scheme through the use of check valves or other circuit-switching approaches would be necessary to maintain unidirectional flow through the heat exchangers for both heating and cooling duty. If refrigerant flow has to be reversed in the heat exchangers, a crossflow heat exchanger with enough rows (as yet undetermined but probably four or more) to approach the performance of the many-row unmixed crossflow case would be required.[9] A requirement for multi-row coils (four or more) for both

---

[9]As the many-row, single-pass crossflow configuration already incurs a significant loss relative to counterflow, it would be important to closely approach this performance to minimize further losses.

HXs could negatively impact the fan power requirements as noted by Hughes (1991) unless a different type of fan were used that handled higher external pressure drops more efficiently.

Relative COP Gains—All Conditions—Counterflow HXs The potential COP gains of ideal mixtures are summarized in Figure 7 for the four air-to-air heat pump conditions of Table 1. Counterflow is assumed in all cases. As in Figure 6, the pure refrigerant baseline (0%) always has the same total system UA as the mixture. The single- and variable-speed 82°F (27.8°C) air-to-air conditions show the most potential of the cases considered—with a 20% COP gain for three times the baseline UA level (or twice the state-of-the-art level). The 95°F (35°C) cooling and 35°F (1.7°C) heating cases follow with 15% and 10%, respectively.

Qualifications to the Predicted COP Gains While the theoretical potential for COP gain shown in Figure 6 for air-to-air heat pumps is encouraging, especially for the cooling mode, close approaches to counterflow HXs and ideal glide matching are important requirements.

Relative to Existing HX Configurations When existing one- and few-row crossflow and counterflow HX configurations are factored into the analysis (based on the effects shown in Figure 5), the maximum COP potential for air-to-air heat pumps narrows considerably. Water-cooled chillers, although they have smaller external(water)-side glides (typically 10° to 12°R [5.5 to 6.7 K]) and thereby less theoretical Lorenz cycle potential, may be more amenable to redesign to approach counterflow than air-to-air units and also have unidirectional refrigerant flow.

Relative to Realistic Glide Matching in Conventional Equipment The second caveat is the assumption of ideal glide matching on both heat exchangers. Departures from this assumption in the simple vapor-compression cycle will

further penalize mixture performance in the heating mode as described by Webb and DiGiovanni (1989) and in low-speed cooling-mode operation. The effects of deviations from ideal glide matching are most significant for these conditions. In both cases, from Table 1, the external fluid glides across the indoor and outdoor coil differ by a factor of three. For a mixture of fixed constituent concentrations, the available refrigerant glides in the evaporator and the condenser are about equal. Therefore, if the mixture concentration is selected to match the larger evaporator air-side glide, the refrigerant in the condenser will overglide relative to the air temperatures and cause the condenser pressure to be elevated. A modified Carnot analysis to determine the fixed refrigerant glide that yields the highest COP over the cooling and heating modes is recommended to quantify the mixture COP overestimate resulting from the assumption of exact glide matching in both HXs.

The extreme glide mismatch conditions would benefit most from the use of a solution circuit (Radermacher 1986; Buschmeier et al. 1990) or other schemes to allow the refrigerant glide to be tailored for each heat exchanger. Water chillers usually have about the same glides on both coils and therefore represent a more compatible application in which to approach ideal glide matching with a mixture of fixed composition.

Relative to Axial Conduction Effects One further consideration is the possible negative effect of increased HX axial conduction across the continuous fin construction of tube-and-fin HXs. This is a potential problem due to the larger refrigerant-side glides required to obtain maximum Lorenz cycle benefits relative to the internal-fluid glides of typical chiller or water-to-air fan coils. Analyses such as those conducted by Chiou (1978) could be used to assess the degree to which axial conduction could result in degradation of crossflow and counter-crossflow HX performance from the levels assumed here.
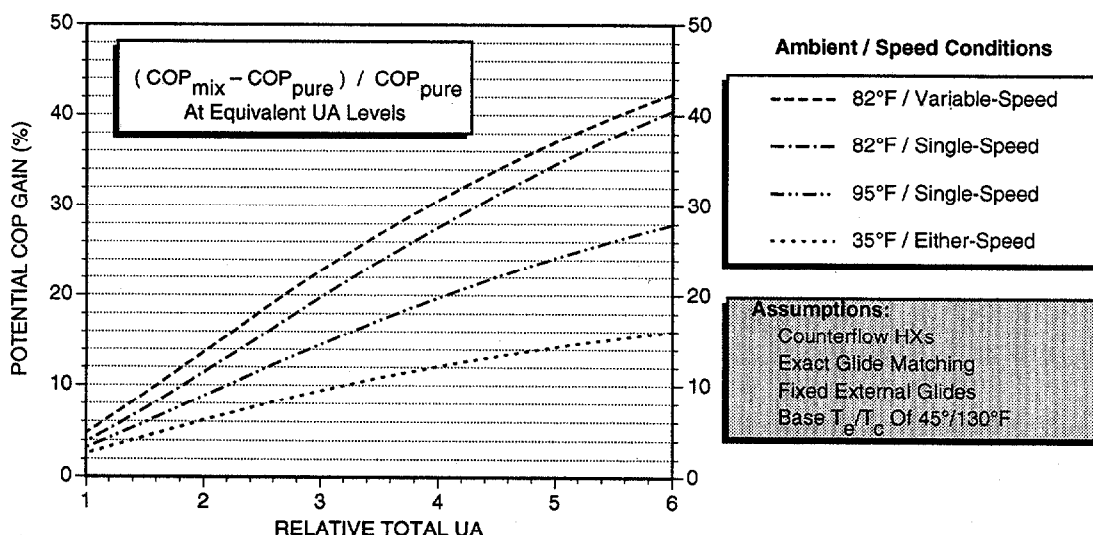

Figure 7   *Maximum potential COP gains from ideal mixtures for unitary air-to-air heat pumps—all conditions.*

Benefits of Refrigerant-Side Heat Transfer Augmentation

The analysis to this point has considered the benefits of larger effective HXs without regard for how the larger total UA multiples might be obtained. In the remaining analysis, we consider how augmentation (or degradation) of the refrigerant-side heat transfer coefficients in evaporators and condensers would affect overall UA values and the idealized application COPs.

Three factors that will reduce the potential gains from refrigerant-side augmentation are

1. air-side-dominant heat transfer resistance (low F_R factors),
2. low external glides on both heat exchangers, and
3. high pressure ratio operation, which can be determined from the refrigerant conditions involved.

The first of these factors relates to both pure and mixed refrigerant cycles and the latter two factors negatively impact the cycle potential with mixtures.

Augmentation Equations From the definition of the refrigerant-side resistance ratio, $F_{R,BASE}$, given by Equation 14 and the relationship between refrigerant, external, and overall UA for each heat exchanger given by Equation 15, an equation relating refrigerant-side augmentation to overall UA multiples can be derived. Let $M_{R,AUG}$ be defined as the refrigerant-side augmentation (or degradation) multiplier. Then the overall UA multiplier for the heat exchanger, $M_{HX,AUG}$, can be related to $F_{R,BASE}$ and $M_{R,AUG}$, using Equations 15 and 16, by

$$M_{HX,AUG} = 1/\{1 - F_{R,BASE} \cdot (1 - 1/M_{R,AUG})\} \quad (16)$$

where the baseline and maximum UA multiples are

$$M_{HX,AUG} = 1, \qquad \text{if } M_{R,AUG} = 1$$
$$M_{HX,AUG} = 1/(1 - F_{R,BASE}), \qquad \text{if } M_{R,AUG} = \infty.$$

For example, for an HX with initially equal air-to-refrigerant-side resistances, i.e., $F_{R,BASE} = 0.5$, the maximum UA multiple increase from refrigerant-only augmentation is a factor of two, whereas with $F_{R,BASE} = 0.25$, the maximum augmentation multiplier is only 1.33. This sample calculation indicates that for refrigerant augmentation to be most beneficial—especially where $F_{R,BASE} < 0.5$—the air-side coefficients must be increased along with the refrigerant-side.

The resulting overall UA multiplier for each heat exchanger is applied to the unaugmented MTD_B by the equation

$$MTD_{AUG} = MTD_B/M_{HX,AUG}. \quad (17)$$

Augmentation Cases *The effects of refrigerant-side augmentation are considered for air-to-air heat pumps at* *the conditions most favorable to mixtures*[10]*—the single-speed, mild-ambient cooling-mode case with counterflow HXs. Both pure and mixed refrigerant augmentation were considered. For the pure refrigerant case, 0% and 100% augmentation levels were evaluated. (Values of $M_{R,AUG}$ were 1.0 and 2.0, respectively). For the mixture analysis, three cases were examined: a worst-case 50% maximum degradation, a break-even case equal to the pure refrigerant heat transfer coefficient, and a 100% past-break-even augmentation. Values of $M_{R,AUG}$ were 0.5, 1.0, and 2.0.

Two levels of initial refrigerant-side resistance ratios were used, corresponding to the lowest and highest $F_{R,BASE}$ estimates provided by the ARI survey. The *low* sensitivity (air-side dominant) case used $F_{R,BASE}$ values of 0.25 for the evaporator and 0.30 for the condenser. The *high* sensitivity (neither-side dominant) case used $F_{R,BASE}$ values of 0.5 for both evaporator and condenser.

Augmentation Results The refrigerant-side augmentation potential of the example cases are shown in Figures 8 and 9 where COP gain percentages are plotted versus relative UA multiples. These two figures show the COP maximum gains possible for the low- and high-sensitivity air-to-air cases, respectively. The individual curves in Figures 8 and 9 show the COP effect of changes in overall UA with equal augmentation on both sides (i.e., while maintaining fixed F_R values). The comparison between curves in a pure or mixed refrigerant family shows the impact of different refrigerant-side augmentation (and degradation) scenarios.[11]

The abscissa and ordinate of Figures 8 and 9 differ from those of Figures 6 and 7 in two significant ways. First, the relative total HX UA is referenced to the *state-of-the-art* size rather than to the low-efficiency baseline used for Figures 6 and 7. Second, the COP gains in Figures 8 and 9 are computed relative to the pure refrigerant COP value *at the state-of-the-art size rather than* relative to the pure refrigerant values *at equivalent UA levels*. Therefore, the two figures show potential COP benefits relative to an unaugmented pure refrigerant case of state-of-the-art HX size.

Discussion The augmentation results for the pure refrigerants show diminishing returns in all cases. For the mixed-refrigerant cases, the 100% (past break-even) augmentation benefits hold constant at about 10 percentage points for the low-sensitivity case (Figure 8) and rise to 20 percentage points with the more balanced resistance ratio (Figure 9). The 50% degradation case lowers the potential mixture COP gain by about 1.5 times the effect of the 100% augmentation. This occurs because a refrigerant-side

---

[10]Conditions that are also most closely represented by the simplifying glide assumptions of the present analysis.

---

[11]Note that only for the $M_{R,AUG} = 1.0$ curves do the F_R ratios remain at the initial values. For the $M_{R,AUG} = 0.5$ and 2.0 cases, the new F_R ratios are given by $F_R = F_{R,B} \cdot M_{HX,AUG}/M_{R,AUG}$.
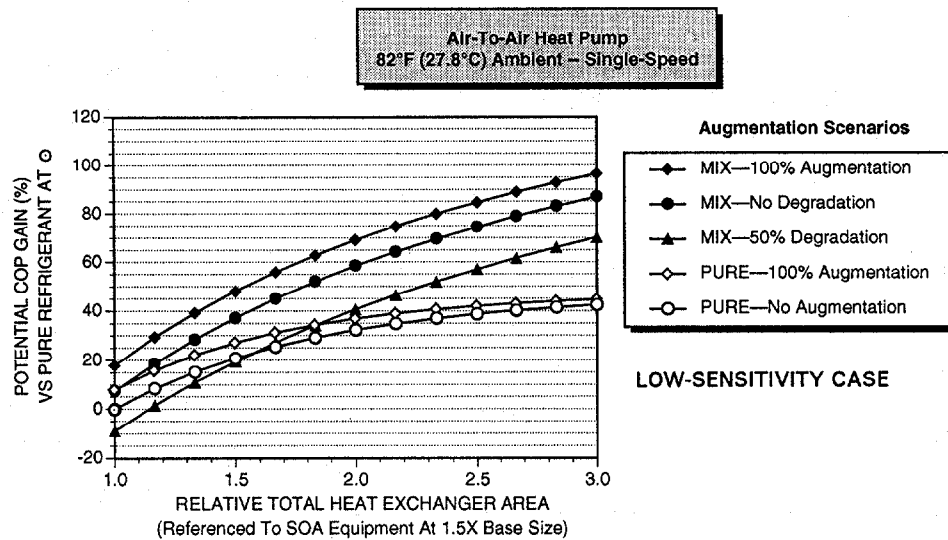
Figure 8 *Refrigerant-side augmentation potential for pure refrigerants and ideal mixtures in air-to-air heat pumps—low-sensitivity case.*
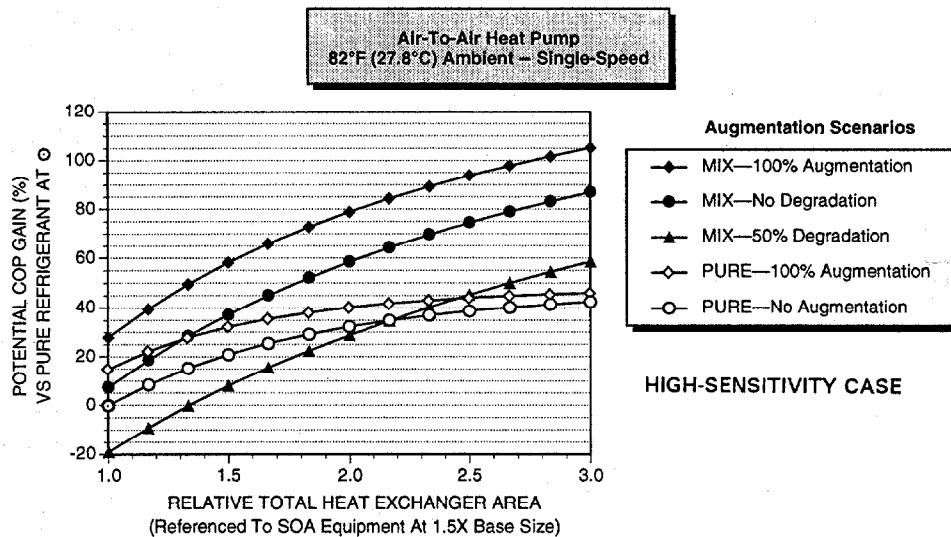

Figure 9 *Refrigerant-side augmentation potential for pure refrigerants and ideal mixtures in air-to-air heat pumps—high-sensitivity case.*

degradation tends to make refrigerant-side effects more dominant on overall UA, while augmentation of the lesser resistance side has more of a dampened effect. Because in neither of the two figures are the dominant resistances on the refrigerant side, it is more effective to first use refrigerant-side augmentation to minimize any mixture heat transfer degradations. Once the break-even heat transfer level is reached, refrigerant- and air-side augmentations should be made simultaneously, whenever possible.

At state-of-the-art UA levels, the postulated 50% maximum degradation level for mixtures is seen to reduce COP in the air-side-dominated case of Figure 8 by about 10% compared to 20% for the neither-side-dominant

(balanced) HX case. Similarly, the crossover HX area (where the mixture COP with $M_{R,AUG} = 0.5$ exceeds that of the pure refrigerant case) needed to compensate for this worst-case heat transfer loss is about 1.6 times state-of-the-art levels for the air-side-dominated case versus 2.2 for the balanced HX. Clearly, mixtures with degraded heat transfer performance are best used in heat pumps with air-side-dominated HXs. Conversely, the best advantage can be made of mixtures and refrigerant-side augmentation when used in balanced- to refrigerant-side-dominant HXs with augmentation that either minimizes, equals, or exceeds the heat transfer performance of the pure refrigerant alternatives.

Figures 8 and 9 can additionally be used to examine the effects of increased coil area (directly proportional to the abscissa) relative to refrigerant-side augmentation (by interpolated movement between the family of curves in the y-direction). The COP sensitivity to the x-axis can alternatively be interpreted as showing the effects of increased overall U as both the air side and refrigerant side are augmented equally while the $F_{R,BASE}$ ratio is maintained.

Increases in effective HX size using advanced refrigerant- and air-side surfaces (movement along the abcissa in Figures 8 and 9 by whatever combinations of overall coil conductance and area are most economical) are seen to benefit preferentially mixture systems that can approach ideal glide matching. Because the economics of heat exchanger design tradeoffs are beyond the scope of this study and nonideal glide-matching effects have not been included, no attempt is made here to identify how much more UA can be economically justified in a mixture system. However, the performance increases predicted by Figures 8 and 9 do suggest that such mixture cycles would have larger UA levels in an economically optimum configuration than their pure refrigerant alternatives.

CONCLUSIONS

Using a modified Carnot analysis with finite HX sizes, counterflow HXs, and ideal glide matching, the potential of the simple vapor-compression Lorenz cycle with refrigerant mixtures was determined for air-to-air heat pump application. The potential COP gains are 1.5 to 2 times larger in the cooling mode than in heating. Maximum COP increases of 8% at state-of-the-art HX sizes and 20% at twice state-of-the-art levels are predicted under single- and variable-speed mild ambient cooling conditions—relative to pure refrigerant performance at equal UA levels.

The effect of deviations from counterflow in the heat exchangers is examined. Counter-crossflow arrangements with two and three rows provide about 50% and 75%, respectively, of the COP performance gain predicted for counterflow—the latter of which is closely approached by coils with four or more counter-crossflow rows.

Losses from many-row crossflow performance relative to counterflow are seen to eliminate or sharply reduce most of the predicted COP gains until a UA multiple of twice state-of-the-art HX size is reached. Few-row crossflow configurations will further lower the relative mixture performance. A counter-crossflow arrangement with two rows is predicted to outperform a many-row crossflow arrangement at UA multiples of most practical interest. This same two-row counter-crossflow arrangement would also outperform a unit with a one-row outdoor coil combined with a four-row counter-crossflow indoor coil.

Means should be further investigated to enable heat pumps using glide-matching mixtures to operate with unidirectional refrigerant flow. Under such conditions, a two-row counter-crossflow outdoor coil combined with a four-row counter-crossflow indoor coil could exceed 75% of the performance potential predicted for heat pumps with counterflow HXs.

Refrigerant-side augmentation with pure refrigerants shows diminishing returns relative to ideally glide-matched mixtures. For glide-matched mixed refrigerants, the COP benefits of 100% augmentation remain constant at about 10 percentage points (relative to a pure refrigerant at the state-of-the-art UA level) for the case of dominant air-side resistance and are near 20% for coils with initially balanced air- and refrigerant-side resistances. Because refrigerant-side heat transfer is not the dominant coil resistance, refrigerant-side-*only* augmentation is most beneficial when used to offset mixture heat transfer degradations.

RECOMMENDATIONS

The modified Carnot approach is proposed as a convenient screening tool for looking broadly at the maximum potential benefits of increased HX area and refrigerant-side augmentation in candidate applications. Modifications should be made to further extend its utility to less idealized cases, such as few-row crossflow configurations and nonideal glide matching. Mixture COP gains predicted from this extended version should be compared to results for specific mixtures with a range of glides in a vapor-compression cycle to establish how well the trends of the simplified approach are correlated.

ACKNOWLEDGMENTS

REFERENCES

Alefeld, G. 1987. Efficiency of compressor heat pumps and refrigerators derived from the second law of thermodynamics. *International Journal of Refrigeration* 10(6): 331-341.

ARI. 1989. *ARI Standard, 210/240-89, Standard for unitary air-conditioning and air-source heat pump equipment.* Arlington, VA: Air Conditioning and Refrigeration Institute.

ARI. 1990. *ARI Standard 520-90, Standard for positive displacement refrigerant compressors, compressor units and condensing units.* Arlington, VA: Air Conditioning and Refrigeration Institute.

Buschmeier, M., W. Mulroy, and D. Didion. 1990. *An initial laboratory evaluation of a single solution circuit cycle for use with nonazeotropic refrigerants.* NISTIR 4406, August. Gaithersburg, MD: National Institute of Standards and Technology.

Chiou, J.P. 1978. The effect of longitudinal heat conduction on crossflow heat exchanger. *Transactions of the ASME* 100: 346-351.

Didion, D.A., and D.B. Bivens. 1990. Role of mixtures as alternatives to CFCs. *International Journal of Refrigeration* 13(May).

Domanski, P.A., and M.O. McLinden. 1990. Performance rating of refrigerants and refrigerant mixtures through simplified cycle calculations. *Proceedings of the 1990 USNC/IIR Purdue Conference,* July 17-20.

Herold, K.E. 1989. Performance limits for thermodynamic cycles. *Proc. of ASME Winter Annual Meeting,* San Francisco, AES-Vol. 8, pp. 41-45.

Hiller, C.C., and L.R. Glicksman. 1976. *Improving heat pump performance via compressor capacity control—Analysis and test,* vol. 2. MIT Laboratory Report No. MIT-EL 76-001.

Holman, J.P. 1972. *Heat transfer,* 3d ed. New York: McGraw-Hill.

Hourahan, G.C., and K. Hickman. 1991. Personal correspondence from G. Hourahan summarizing results of ARI member survey in response to ORNL request for industry input, November.

Hughes, H.M. 1991. Refrigerant blends: The realities. *International CFC and Halon Alternatives Conference,* Baltimore, MD, December 3-5.

Jung, D., and R. Radermacher. 1991. Performance simulation of a two-evaporator refrigerator/freezer charged with pure and mixed refrigerants. *Int. J. Refrigeration* 14(Sept.): 254-263.

Kays, W.M., and A.L. London. 1964. *Compact heat exchangers,* 2d ed. New York: McGraw-Hill.

Kedzierski, M.A., and D.A. Didion. 1991. Personal communication to V.D. Baxter of ORNL regarding an unpublished analysis at NIST, Gaithersburg, MD, April.

Klein, S.A. 1992. Design considerations for refrigeration cycles. *International Journal of Refrigeration* 15(3): 181-185.

Kondepudi, S.N., and A.A. Bhalerao. 1992. A parametric analysis on the seasonal heating coefficient of performance (SHCOP) of air to air heat pumps. *Recent Research in Heat Pump Design, Analysis, and Applica-*

tion, AES-Vol. 28, pp. 79-87. American Society of Mechanical Engineers.

Lorenz, H. 1894. Die Ausnutzung der Brennstoffe in den Kuhlmaschinen. *Zeitschrift fur die gesammte Kalte Industrie,* Vol. 1, pp. 10-15.

McLinden, M.O. 1990. Optimum refrigerants for non-ideal cycles: An analysis employing corresponding states. *Proceedings of the 1990 USNC/IIR Purdue Conference,* pp. 69-79, July 17-20.

McLinden, M.O., and R. Radermacher. 1987. Methods for comparing the performance of pure and mixed refrigerants in the vapor compression cycle. *Int. J. Ref.* 10(Nov.): 318-325.

Pannock, J., and D.A. Didion. 1991. The performance of chlorine-free binary zeotropic refrigerant mixtures in a heat pump. NISTIR 4748, December. Gaithersburg, MD: National Institute of Standards and Technology.

Pannock, J., D.A. Didion, and R. Radermacher. 1992. Performance evaluation of chlorine-free binary zeotropic refrigerant mixtures in heat pumps—Computer study and tests. *Proceedings of the 1992 International Refrigeration Conference—Energy Efficiency and New Refrigerants,* D.R. Tree, ed., Purdue University.

Radermacher, R. 1986. Advanced versions of heat pumps with zeotropic refrigerant mixtures. *ASHRAE Transactions* 92(2A): 52-59.

Rice, C.K. 1991. *The ORNL modulating heat pump design model—User's guide.* ORNL/CON-343, Draft Report, June. Oak Ridge, TN: Oak Ridge National Laboratory.

Rice, C.K. 1992a. Benchmark performance analysis of an ECM-modulated air-to-air heat pump with a reciprocating compressor. *ASHRAE Transactions* 98(1).

Rice, C.K. 1992b. *Level 1 sensitivity analysis of HRAC heat exchanger enhancement benefits.* ORNL Task Report for DOE Office of Building Technologies, June. Oak Ridge, TN: Oak Ridge National Laboratory.

Rice, C.K., and J.R. Sand. 1990. Initial parametric results using CYCLEZ—An LMTD specified, Lorenz-Meutzner cycle refrigerator-freezer model. *Proceedings of the 1990 USNC/IIR Purdue Conference,* pp. 448-458, July 17-20.

Stevens, R.A., J. Fernandez, and J.R. Woolf. 1957. Mean temperature difference in one, two, and three-pass crossflow heat exchangers. *ASME Transactions* 79: 287-297.

Vineyard, E.A., J.C. Conklin, and A. Brown. 1993. Cycle performance testing of nonazeotropic mixtures of HFC-143A/HCFC-124 and HFC-32/HCFC-124 with enhanced surface heat exchangers. *ASHRAE Transactions* 99(1).

Webb, R.L., and M.A. DiGiovanni. 1989. Comparison of mixture and pure refrigerant heat pump cycles. *Heat Recovery Systems & CHP* 9(4): 383-396.